Energy levels in quantum wells with capping barrier layer of finite size: Bound states and oscillatory behavior of the continuum states

S. Fafard
Department of Physics, Ottawa-Carleton Institute for Physics, University of Ottawa, Ottawa, Ontario, Canada K1N 6N5
(Received 20 January 1992; revised manuscript received 18 May 1992)

The problem of a quantum-well structure in the vicinity of a high potential was studied theoretically. This problem corresponds to real devices with a finite-size capping layer. Results are obtained for the bound and the continuum states of a single quantum well, the continuum states of a multiple quantum well (MQW), and the continuum states with an electric field applied to the structure. For the bound states with no electric field, an equation including the cap-layer thickness (i.e., the distance of the well from the high potential) as one of its parameters is derived, and solved numerically for various well widths and cap-layer thicknesses, showing that significant deviations from the "regular" quantum-well levels are only expected for very thin cap layers (of the order of about 10 nm). The wave functions of the continuum states are found analytically, and used to calculate the probability of finding the carriers in the various regions of the device [cap layer, well(s), or buffer]. The theory predicts large energy-dependent oscillations in these probabilities for energies ranging up to more than 100 meV in the continuum; their periods depend on the cap-layer thickness and the carrier effective mass. Carrier segregation is then expected among the various regions for energies above the confining barriers. The contrast in probability between the regions increases for thin wells, deep potentials, and small effective masses, and is also enhanced by the presence of additional wells in the case of MQW's. For MQW's, the theory also predicts that the well(s) nearest to the surface will be more energy selective in capturing carriers in the continuum. This may result in different capture efficiencies for the various wells of a MQW structure. If an applied electric field lowers the potential away from the surface of the structure, the probability peaks shift linearly in energy with the magnitude of the field, and for small energies above the continuum edge, the probability of finding carriers in the well region increases.

I. INTRODUCTION

Recent experimental evidence[1] has shown that the ideal quantum-well potential in which a quantum well is considered to be surrounded by barriers of finite height, but infinite in extent on each side, must be modified to take into account the finite thickness of the cap layer when a thin cap layer is used in actual semiconductor quantum-well devices. If the carriers diffuse coherently throughout the device, remote interfaces can become an important part of the potential configuration. Thus, if a thin cap layer is used, the energy distribution of carriers around the well may be modified by the presence of the external surface, which represents a high potential for the carriers inside the semiconductor. The influence of the surface potential will be more important for the continuum states than for the bound states because their wave functions are not restricted to the well region. These continuum states play a crucial role, because when energies larger than the barrier are used, they are the energy levels in which the carriers are first excited before they relax to the fundamental levels in the well(s).

The influence of a high potential in the vicinity of a quantum-well structure will be considered theoretically. Such a configuration would represent an actual quantum-well device having a cap layer of finite size. It will be assumed that the external surface of the cap layer will represent an infinitely high potential (see Fig. 1). This will be a good assumption for energies up to a few hundred meV in the continuum, given that the actual height of the surface potential is of the order of several electron volts (the work function of the carriers in the semiconductor). The envelope function will be required to vanish at the surface. This will be valid for the treatment of an ideal free surface, and merely illustrates the fact that for the energy range of interest, the carriers cannot escape the semiconductor crystal. The model developed here would also apply to quantum-well structures terminated with a material having a band gap much larger than the barriers (such as $Al_xGa_{1-x}As/GaAs/In_xGa_{1-x}As/GaAs$), even though these structures will not be discussed specifically in this paper. The presence of surface states would change the problem, but once these localized states are filled, this problem could also be solved by assuming that the envelope wave function vanishes at the surface, taking into account the resulting band curvature. For simplicity, this paper will consider only the potentials depicted in Fig. 1, but band curvature could be considered in more elaborate calculations by approximating the curved potential with a series of small linear potential segments.

The theoretical predictions are illustrated with examples for an $In_xGa_{1-x}As/GaAs$ system. The theory is in no way restricted to that system, but since the barrier is

the GaAs, the samples are naturally barrier terminated, and chances of getting a nearly perfect external surface (GaAs cap layer) are greater than if an alloy is used for the barrier, as in the $Al_xGa_{1-x}As/GaAs$ system, for example. The $Al_xGa_{1-x}As/GaAs$ samples often have a GaAs cap layer on top of the $Al_xGa_{1-x}As$ barrier, and this would correspond to a different potential configuration.

The theory uses parabolic bands for simplicity; and the envelope-function approximation reduces the problem to solving the one-dimensional (1D) Schrödinger equation for the given potential, by matching at the interfaces the wave function and its derivative divided by the effective masses of the material (i.e., the particle current density). Results are presented first for the bound states of a single quantum well (SQW) at a distance t from a high potential. An equation is derived and solved numerically giving the well-width dependence of the energy levels for various cap-layer widths (i.e., the distance from the high potential). Then, the continuum-state wave functions are found, and the probability density is integrated to calculate the probability of finding the carriers in the various regions of the device. The theory is then generalized for the continuum states of multiple quantum wells (MQW's). Finally, the continuum states are studied with an applied electric field which lowers the potential away from the surface of the structure.

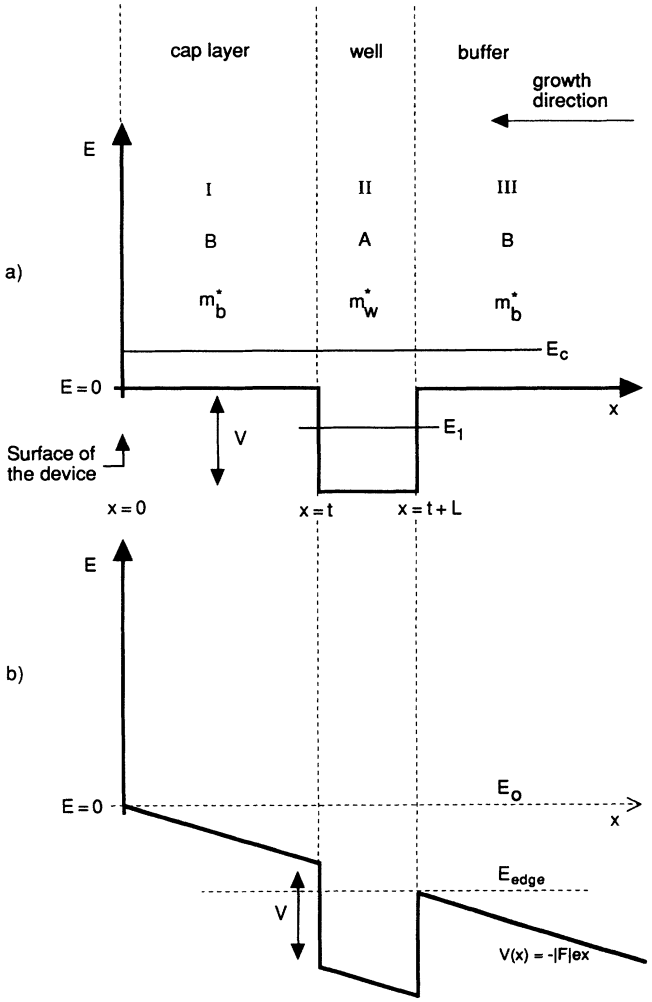

FIG. 1. SQW with capping barrier layer of finite size; cap of width t, well of width L and depth V, and thick buffer layer. (a) Band diagram showing the high potential at the surface at $x=0$. (b) Band diagram when an applied electric field lowers the potential away from the surface. E_{edge} is the energy at which the continuum states start.

II. THEORETICAL RESULTS

A. SQW bound states ($E<0$); no applied field ($|F|=0$)

Figure 1(a) shows the band diagram for a SQW with a finite cap-layer of width t. The potential is assumed infinitely high for $x\leq 0$, and so it is required that $\Phi(0)=0$. Therefore the solution of the Schrödinger equation in the cap layer takes the form $\Phi_I(x)\propto \sinh\gamma x$, and the condition for the bound states is readily obtained:

$$2\cos kL=\sin kL[(1/\xi-\xi)-e^{-2\gamma t}(1/\xi+\xi)]\ . \qquad (1)$$

Where L is the well width, and if the energy is measured from the bottom of the well, say $\varepsilon=|V|-|E|$, then

$$k=\left[\frac{2m_w^*}{\hbar^2}\varepsilon\right]^{1/2},\quad \gamma=\left[\frac{2m_b^*}{\hbar^2}(|V|-\varepsilon)\right]^{1/2},$$

and

$$\xi=\left[\frac{m_w^*}{m_b^*}\frac{(|V|-\varepsilon)}{\varepsilon}\right]^{1/2};$$

m_b^* and m_w^* are the barrier and well effective masses, respectively.

Equation (1) has two limiting cases of interest: (a) for large t (i.e., a regular SQW), it reduces to the well-known[2-4] equations for regular SQW's, $\xi=\tan kL/2$ and $-\xi=\cot gkL/2$, for the even- and the odd-parity levels respectively; (b) $t\to 0$, i.e., a semi-infinite SQW, leads to $-\xi=\cot gk(2L)/2$, which gives the odd levels only of a regular SQW twice as wide. This is expected since the odd levels of a regular SQW twice as wide will always have a node at their center, just as the semi-infinite SQW will have a node (the wave function is terminated) at the surface. Since only the odd levels are present, there will be no bound states for $L<(\pi\hbar)/2(2m_w^*V)^{1/2}$ (i.e., until the second level appears in the regular well of twice the width having the same potential depth).

Between these limiting cases, Eq. (1) was used to calculate the influence of the cap-layer thickness t on the bound-energy levels of SQW's. Figure 2 gives an example of results for a system having confining energies $V^e=121$ meV and $V^{hh}=60$ meV for the electrons and heavy holes, respectively, for well widths ranging from 0 to 10.0 nm. The effective masses were taken to be $m_w^*=m_b^*=0.0665m_0$ for the electrons and $m_w^*=0.37m_0$, $m_b^*=0.41m_0$ for the heavy holes. Those values correspond to an $In_{0.16}Ga_{0.84}As/GaAs$ system. The solid lines are for the regular SQW (i.e., $t\to\infty$). The dash-dotted line is for the semi-infinite QW (i.e., $t=0$). The two lines

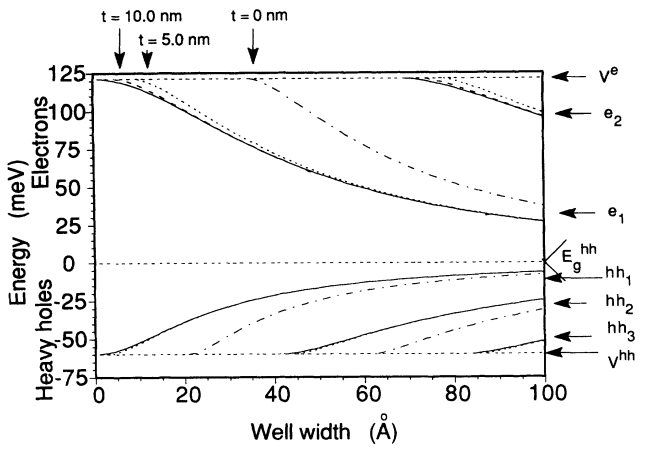

FIG. 2. Well-width dependence of the bound states of a SQW as in 1(a) for various values of cap-layer thicknesses. The system chosen has for the electrons (top part of the figure) $V^e=121$ meV; $m_w^*=m_b^*=0.0665m_0$ and for the heavy holes (bottom part of the figure) $V^{hh}=60$ meV; $m_w^*=0.37m_0$ and $m_b^*=0.41m_0$. The horizontal line at $E=0$ represents the bottom of the wells (the electrons and heavy holes are separated by the heavy-hole band gap E_g^{hh}). The horizontal lines at the V's represent the onset of the continua. Two electron levels (e_1 and e_2) and three heavy-hole levels (hh_1,hh_2, and hh_3) are shown by the curves, for four cap-layer thicknesses: The solid line is for the regular SQW ($t\to\infty$), the dash-dotted line is for the semi-infinite quantum well ($t=0$), the other two curves in between (often superposed to the solid line) are for $t=10.0$ and 5.0 nm. (These values of potentials and effective masses would correspond to an $In_{0.16}Ga_{0.84}As/GaAs$ system at 4.2 K.)

in between are for $t=10.0$ and 5.0 nm. For $t\gtrsim 10.0$ nm, there is practically no deviation from the regular SQW results, because unless the well width is such that the level is just below the confining potential V (i.e., small γ), the $e^{-2\gamma t}$ term of Eq. (1) will be small (i.e., the wave function in the barrier dies off fairly quickly for typical values of $|V|-\varepsilon$ and m_b^*). One also notes that the effect is smaller for the heavy holes because of their larger effective mass. For small t, however, the shifts in the energy levels are quite significant and one could not neglect this effect if such a device were to be built.

B. SQW continuum states ($E\geq 0$); no applied field ($|F|=0$)

To understand the behavior of the carriers in the continuum states, the wave function is constructed by also requiring $\Phi(0)=0$, so that here

$$\Phi_{\rm I}(x)\propto \sin k_b x\ ,$$

$$\Phi_{\rm II}(x)=A\sin k_w(x-t)+B\cos k_w(x-t)\ , \tag{2a}$$

$$\Phi_{\rm III}(x)=C\sin k_b[x-(t+L)]+D\cos k_b[x-(t+L)]\ ,$$

where $\hbar^2k_b^2/2m_b^*=E$, $\hbar^2k_w^2/2m_w^*=E+|V|$, and the coefficients of Eq. (2a) are

$$A=\xi\cos k_b t,\quad B=\sin k_b t\ ,$$
$$C=\cos k_b t\cos k_w L-1/\xi\sin k_b t\sin k_w L\ , \tag{2b}$$
$$D=\xi\cos k_b t\sin k_w L+\sin k_b t\cos k_w L\ ,$$

here, $\xi=k_b m_w^*/k_w m_b^*$. After the integration of the probability density $[|\Phi(x)|^2]$ found from Eq. (2), we get

$$p_c=\frac{t}{2}\left[1-\frac{\sin 2k_b t}{2k_b t}\right]\ , \tag{3a}$$

$$p_w=\frac{L}{2}\left[(A^2+B^2)+(B^2-A^2)\frac{\sin 2k_w L}{2k_w L}+2AB\frac{\sin^2 k_w L}{k_w L}\right]\ , \tag{3b}$$

$$p_b=\frac{x_{\max}}{2}\left[(C^2+D^2)+(D^2-C^2)\frac{\sin 2k_b x_{\max}}{2k_b x_{\max}}+2CD\frac{\sin^2 k_b x_{\max}}{k_b x_{\max}}\right]\ , \tag{3c}$$

where p_c, p_w, and p_b are the unnormalized probabilities of finding carriers with an energy E in the cap, well, and buffer regions, respectively. p_w is sometimes referred to as the *well occupancy* [Eq. (3b)], and $x_{\max}$ in Eq. (3c) is the upper bound at which the integration is truncated. The truncation of the integral will not reduce the accuracy of the results if $x_{\max}\gg t+L$. Since the buffer layer will be much thicker than the cap layer, the thickness of the buffer layer can be taken for the value of $x_{\max}$. The substrate region (i.e., the material beneath the first-grown barrier) is not considered in the calculations because it is often doped or of poorer quality. Hence, the coherence of the wave function will be lost after a short distance, and/or the different doping level can result in the presence of a barrier at the buffer-substrate interface.

The normalized probabilities of finding carriers of energy E in the various regions are obtained by dividing the Eq. (3) by the total probability of finding carriers of energy E in the whole device, i.e., $p_t=p_c+p_w+p_b$. Another quantity of interest, which could be associated with the density of states in the device induced by the presence of the well, is $p_t/p_{\rm box}$, where $p_{\rm box}$ is the unnormalized probability of finding carriers with energy E in the corresponding box without the quantum well:

$$p_{\rm box}=\frac{x_{\max}}{2}\left[1-\frac{\sin 2k_b x_{\max}}{2k_b x_{\max}}\right]\ . \tag{4}$$

Calculations show that $p_t/p_{\rm box}$ behaves like the probabilities of finding the carriers in the various regions given by Eq. (3). Consequently, the following examples will use only the latter quantities.

Of the three terms in Eqs. (3b) and (3c), the first term is usually dominant because of the large denominators in the second and third terms [especially in Eq. (3c)]. Substituting Eqs. (2b) into the first term of Eq. (3c), one obtains

$$C^2+D^3=\cos^2 k_w L+\sin^2 k_w L(1/\xi^2\sin^2 k_b t+\xi^2\cos k_b t)$$
$$+2\cos k_w L\sin k_w L\cos k_b t\sin k_b t(\xi-1/\xi)\ .$$

The well width L is usually relatively small compared to the cap-layer thickness t, and so the above term will oscillate with energy as $k_b t$ changes, giving peaks of probability at certain energies in the various regions. When the energy $E\to 0$, $\xi\to 0$, and as E increases, $\xi\to 1$ and $C^2+D^2\to 1$, so that the oscillations of probability with energy disappear at higher energy; then, the system behaves classically. In this situation, the classical probability of finding carriers in any specific region is given by the ratio of the width of the region to the total width of the device.

The best contrast in the probabilities of Eq. (3b) or (3c) is obtained if $k_w L$ is equal to an odd multiple of $\pi/2$ at an energy slightly above the barrier. For that energy, $\cos k_w L=0$, $\sin k_w L=1$, and for energies around this value, the unnormalized probability in the buffer region becomes $p_b\approx 1/\xi^2\sin^2 k_b t+\xi^2\cos^2 k_b t$, so that for small E, $\xi\to 0$ and p_b varies as $\sin^2 k_b t$ which has its extrema (maxima or minima) given by

$$E_n=\frac{\pi^2\hbar^2}{8t^2 m_b^*}n^2\ , \tag{5}$$

where n is an integer. If the buffer layer is thick (large $x_{\max}$), p_b usually dominates p_t because of the $x_{\max}$ factor in Eq. (3c). Therefore, carriers will usually occupy the buffer region except around the minimum of p_b, i.e., when $\sin^2 k_b t$ has a zero; then p_t is dominated by p_c, so that $P_c=p_c/p_t$ is close to unity. This is illustrated in Fig. 3 which shows the normalized probabilities of finding electrons in the cap [Fig. 3(a)], in the well [Fig. 3(b)], and in the buffer [Fig. 3(c)] regions for a cap-layer width of 50.0 nm, a buffer of 1.0 μm, for the system of Fig. 2 (i.e., $V^e=121$ meV, $m_w^*=m_b^*=0.0665m_0$) with a well width of 3.5 nm. The dashed horizontal lines represent the values of the classical probabilities. In Fig. 3(a) one notes that P_c has sharp probability peaks, especially for small E, and outside these "resonance" peaks the probability goes back down close to zero, as explained above for the case $k_w L=\pi/2$ for small E. The values for the first three maxima of probability are 73%, 42%, and 26%, compared to 50.0 nm/1053.5 nm=4.7% for the classical probability of finding the carriers in the cap. This is a remarkable energy segregation of the carriers among the various regions induced by the presence of the high potential at the surface.

Probability peaks similar to those of Fig. 3(a) are also observed for the well region, see Fig. 3(b). The well is narrow compared to the cap and buffer, so that the maximum values of probability in the well are relatively small. As opposed to the situation for the cap, the envelope of the oscillation pattern decreases slowly on a smoothly increasing background to reach the value of the classical probability (3.5 nm/1053.5 nm=0.33%) as E increases. Figure 3(c) (the probability in the buffer) is approximately one minus the values of Fig. 3(a) since the values for the probability in the well are small ($P_c+P_w+P_b=1$). As long as the thickness of the buffer layer is kept large compared to the size of the cap and well regions, the choice of the buffer layer size will only affect the values on the vertical axis of the graphs; indeed, for buffer layer sizes larger than a few times that of the cap layer, the shape of the oscillations is essentially independent of the buffer size. The ratio of the probabilities of finding the carriers in the various regions with the classical probabilities would be independent of the buffer size under these conditions.

Considering the wave function for various values of energy, it is easy to visualize what is happening with the probabilities. Figure 4 depicts the wave function, calcu-

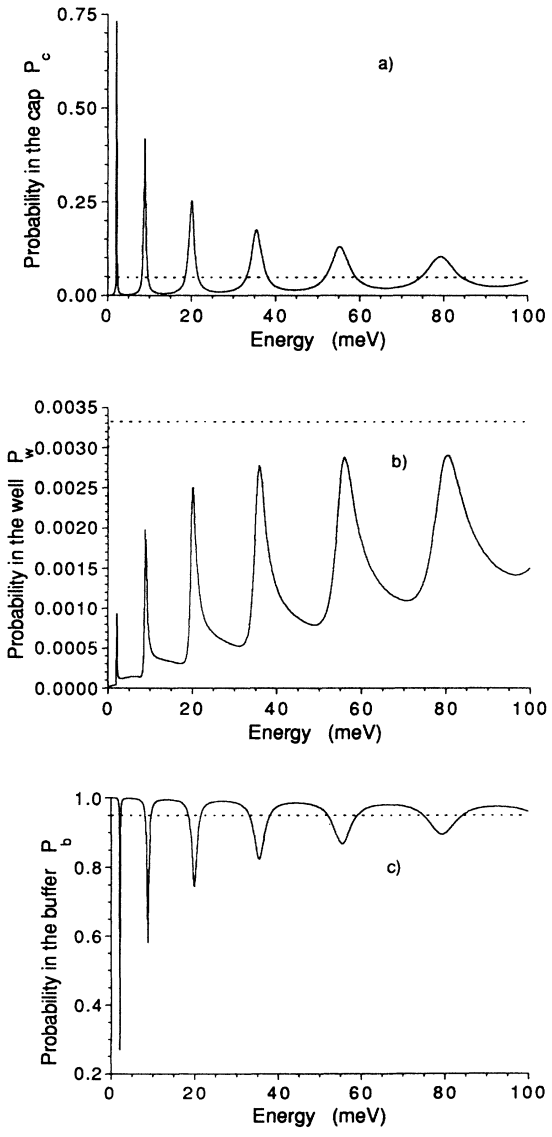

FIG. 3. Energy variations of the normalized probabilities of finding the electrons in the various regions of the SQW of 1(a), for a cap layer of 50.0 nm for the system of Fig. 2 with a well width $L=3.5$ nm. The buffer layer considered was 1.0 μm thick. The dashed horizontal lines are the classical probabilities. (a) is for the cap-layer region, (b) is for the well, and (c) is for the buffer.

lated from Eqs. (2), of the electrons for the example of Fig. 3, for the first two resonant probability peaks of the cap [Figs. 4(a) and 4(b)], and for an off-resonance situation, Fig. 4(c). The wave function for the first peak (at $E=2.25$ meV) has no node in the cap ($x<50.0$ nm), whereas the wave function for the second peak (at $E=8.98$ meV) has a node in the middle of the cap. The ratio of the amplitude of the wave function in the cap to the amplitude of the wave function in the buffer ($x>53.5$ nm) is larger in the first "mode," giving a higher peak of probability in the cap. In the off-resonance case, Fig. 4(c) for $E=4.5$ meV, the wave-function amplitude is much smaller in the cap than it is in the buffer.

The previous example satisfied the condition $k_w L=\pi/2$ for small E, in which case a good contrast in the probabilities is observed. Now to illustrate the case where $k_w L \lesssim \pi$ for small E (i.e., the case in which there would be a "resonant continuum state" for the regular SQW), one may calculate the probabilities for the heavy holes for the same type of well (i.e., $L=3.5$ nm; $t=50.0$ nm; buffer of 1.0 μm, and now $V^{\rm hh}=60$ meV; $m_w^*=0.37m_0$; $m_b^*=0.41m_0$). Indeed, the heavy holes in such a well satisfy the condition $k_w L \lesssim \pi$ for small E. Results are shown in Fig. 5 for the probability in the cap layer [Fig. 5(a)] and in the well [Fig. 5(b)]. The probability for the buffer region is not shown, because it is easily deduced from Fig. 5(a), as explained in the previous example. The spacing between the extrema is smaller for the heavy holes than it was for the electrons in Fig. 3, because of the larger effective mass of the heavy holes [larger m_b^* in Eq. (5) decreases the spacing between the E_n]. In Fig. 5(a) for the cap layer, the first few peaks have probabilities much higher than the classical probability (65%, 36%, and 21% for the first three maxima as compared to 4.7% for the classical probability). However, the contrast of probability is not as large as it was in the previous example, the minima of probability having larger values here. The striking feature in Fig. 5(a) is the node in the envelope pattern of the oscillations at around 24 meV. At this energy, $k_w L=\pi$, and the regular SQW would have a so-called resonant continuum state. This means that a particle incident on one side of the regular SQW has a probability of transmission to the other side equal to unity. Similarly here, if the condition $k_w L=\pi$ is satisfied, the well forms an "open channel" for the carriers in the cap and buffer regions. Consequently, the classical values of probabilities are expected at this energy. Except for the smaller spacing between the extrema of the oscillations, the probabilities of finding the heavy holes in the well [Fig. 5(b)] behave similarly to what was seen for the electrons [Fig. 3(b)].

Situations of good contrast of probability at low energy

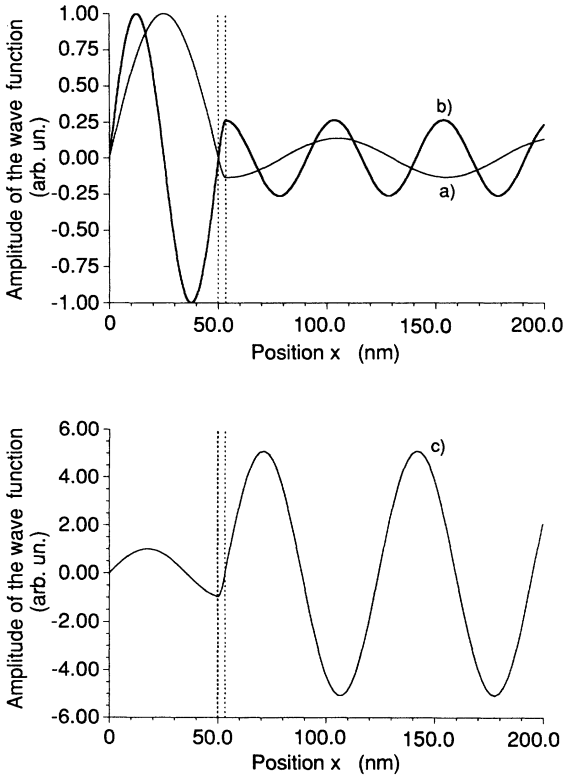

FIG. 4. Amplitude of the wave function throughout the device for the first two probability peaks in the cap layer and for an off-resonance situation for the example of Fig. 3. (a) is for the first peak at $E=2.25$ meV, (b) is for the second peak at $E=9.98$ meV, and (c) is for the off-resonance situation at $E=4.5$ meV. The region between the two vertical dashed lines corresponds to the well of width $L=3.5$ nm; to its left is the cap layer of width $t=50.0$ nm, and to its right the thick buffer.

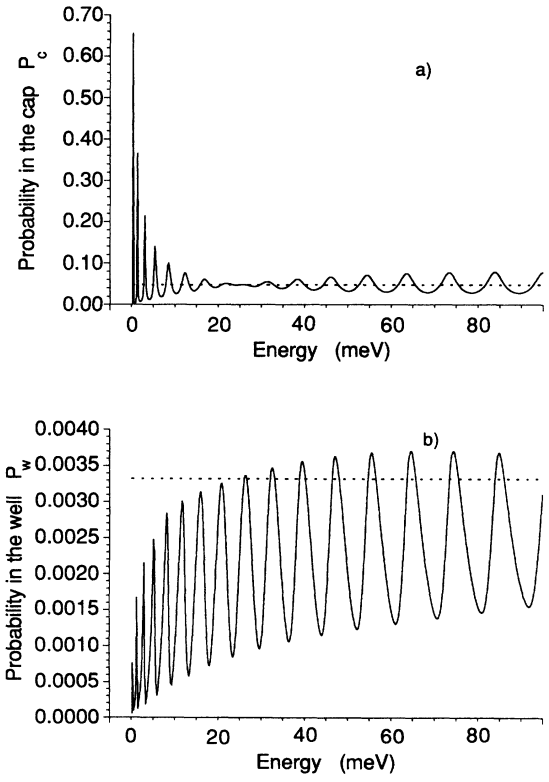

FIG. 5. Energy variations of the normalized probabilities of finding the heavy holes for the structure of Fig. 3, for (a) the cap and (b) well regions. At $E=24$ meV, $k_w(E)L=\pi$.

(like Fig. 3, first example), for the system of Fig. 2, will be obtained for the heavy holes at $L \approx 2.0$, 6.2, 10.3 nm, etc. (i.e., $k_w L = \pi/2$, $3\pi/2$, and $5\pi/2$, respectively). For the electrons, good contrast is obtained for $L \approx 3.4$, 10.2 nm, etc. (i.e., $k_w L = \pi/2$ and $3\pi/2$). For larger well widths however, the argument $k_w L$ changes more rapidly with energy, reducing the energy range in which good contrasts are observed. A situation of open channel or resonant continuum states like Fig. 5 (second example), will be observed if the well width is slightly smaller than the width at which a bound state appears.

The depth of the potential well will influence the way in which ξ reaches unity as E increases. For a shallower potential, ξ is closer to unity for a given energy, and the system behaves more classically (as expected for a shallow potential), giving less probability contrast. The spacing between the extrema of probability is determined mainly by $\sin^2(k_b t)$ which has its extrema given by Eq. (5). Consequently, if the product of the square root of the carrier effective mass and the cap thickness is large, the energy difference between two consecutive extrema of probability becomes small, approaching classical behavior in the limit of "high quantum numbers."

C. MQW continuum states; $|F| = 0$

The case of a double quantum well will be investigated to illustrate the changes in the continuum states induced by additional wells for a MQW structure having a thin cap layer. Two wells like the one of the first example of the preceding section (well width 3.5 nm; $V^e = 121$ meV; $m_w^* = m_b^* = 0.0665 m_0$; the cap layer is 50.0 nm, the buffer 1.0 μm) are separated by $d = 5.0$ nm. The normalized probabilities have been calculated for the various regions ($P_{\text{cap}}, P_1^w, P_1^b, P_2^w, P_b$). Figures 6(a)–6(c) show the probabilities of finding the electrons in the cap layer (P_{cap}), over the first well (P_1^w) and over the second well (P_2^w), respectively. Comparing with Fig. 3 for the SQW, one sees that the probabilities peak at around the same energies, but the peaks are sharper and higher, giving even better contrasts. A remarkable feature in the first well of the DQW (the one closer to the cap) in Fig. 6(b) is that the probabilities at their peaks are higher than the classical probability, in contrast with the SQW in Fig. 3(b), or with the second well of the MQW in Fig. 6(c). And so the first well, closer to the surface, will be more energy selective in capturing carriers in the continuum. This may result in different capture efficiencies for the various wells of a MQW structure. Trial calculations with values other than $d = 5.0$ nm indicate that the sharpest contrasts in the probabilities (sharp peaks with high maxima and low minima) were obtained with small values of $k_b d$ (i.e., $k_b d$ smaller than π for $E \lesssim 100$ meV). Whenever $k_b d$ is equal to a multiple of π, extra features are observed with the probabilities. However, a detailed analysis of all the parameters involved in MQW's in the vicinity of a high potential (or other structures such as the double-barrier potential) is beyond the scope of this paper. Calculations with more than two wells have indicated that the trend described above continues as the number of wells is increased.

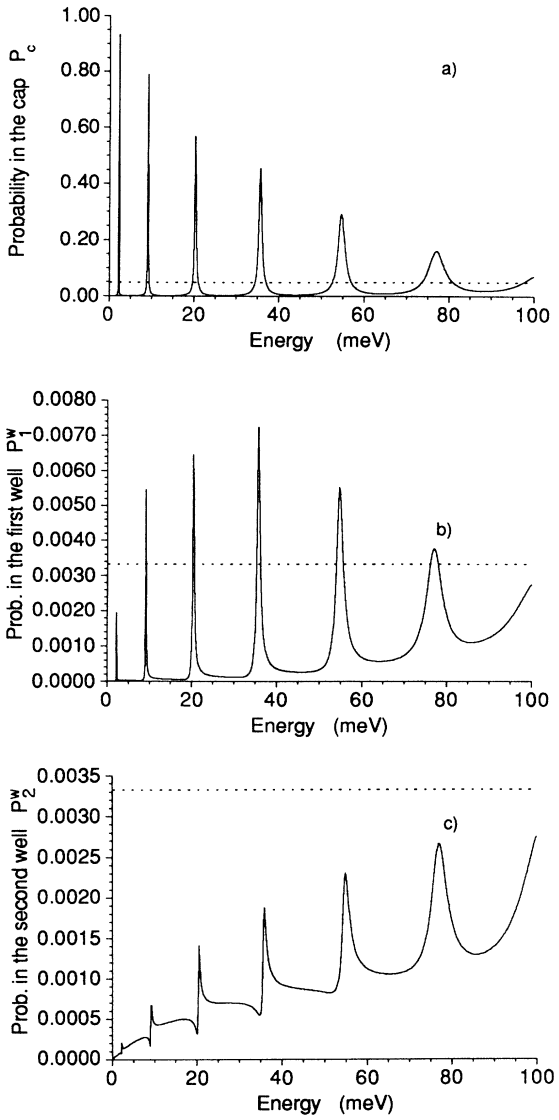

FIG. 6. Energy variations of the normalized probabilities of finding the electrons in the various regions of a double well separated by a barrier of width $d = 5.0$ nm, for the structure of Fig. 3. (a) is for the cap-layer region, (b) is for the first well, and (c) is for the second well. Compare with Fig. 3 for a single well.

D. SQW continuum states with an applied electric field ($E > 0, |F| \neq 0$)

The problem studied in this section is depicted in Fig. 1(b). An electric field (F) is applied to the SQW potential of Fig. 1(a); the polarity of the field is chosen such that the potential away from the surface is lowered. The problem with the other field polarity reduces to that of a quantum well in a triangular potential, and will not be studied here.[5] As before, the cap wave function must vanish at $x = 0$, and so

$$\Phi_{\text{cap}}[z(x)] \propto \text{Bi}[z(0)]\text{Ai}[z(x)] - \text{Ai}[z(0)]\text{Bi}[z(x)] ,$$
$$\Phi_{\text{well}}[\zeta(x)] = \alpha_2 \text{Ai}[\zeta(x)] + \beta_2 \text{Bi}[\zeta(x)] , \quad (6)$$
$$\Phi_{\text{buffer}}[z(x)] = \alpha_3 \text{Ai}[z(x)] + \beta_3 \text{Bi}[z(x)] ,$$

where Ai and Bi are the Airy functions[6] with the arguments

$$z(x)=-x(2m_b^*|F|e/\hbar^2)^{1/3}[1+E/(|F|ex)]\ ,$$

and

$$\zeta(x)=-x(2m_w^*|F|e/\hbar^2)^{1/3}[1+(E+|V|)/(|F|ex)]\ .$$

To illustrate the influence of an applied electric field on the probabilities of finding the carriers in the various regions, calculations were performed for the SQW structure of the example of Fig. 5. Results in Fig. 7 show the evolution of the probabilities for the heavy holes as the applied field F is changed, curves i to xi are the normalized probabilities of finding the heavy holes in the cap layer [Fig. 7(a)], and in the well [Fig. 7(b)] for electric-field values between 0.0 and 10.0 kV/cm, in steps of 1.0 kV/cm. The horizontal axis represents the energy measured from the lower edge of the well [see Fig. 1(b)]. The probability peaks are found to shift monotonically to higher energies as the electric field is increased. To gain more knowledge on these shifts, Fig. 8 compares the 0-kV/cm (curve i) and the 5.0-kV/cm (curve vi) spectra of Fig. 7(b). Curve vi of Fig. 8 was shifted in energy to show that the peaks at positive energies (those to the right of the vertical dashed line, labeled 7–15) correspond to those of the zero-field situation; that is, the spacing between the peaks is preserved, but their positions are shifted in energy with the applied electric field. There are two contributions to that shift: the edge of the well is moved down in energy with increasing electric field, displacing the peaks upward by the same amount [here +5.35 meV/(kV/cm)], and the peaks are shifted because now Eq. (6) determines the oscillations in probability instead of Eq. (2). For the present example, the latter shift is found to be −2.49 meV/(kV/cm), giving a net shift of +2.86 meV/(kV/cm). For $E \geq 0$, the vertical potential limits the structure near the surface, and this is why the peaks in probability are very similar to those found for the zero-field situation: the separation between the extrema increases as the energy is increased; however for $E < 0$, the structure is limited near the surface by the tilted potential, and the peaks in probability get closer together as the energy is increased, as can be seen in Fig. 8, curve vi, to the left of the vertical dashed line. Another remarkable feature induced by the applied electric field is the overall increase in the probability of finding the carriers in the well region at small energies. The zero-field probabilities of finding the carriers in the well were smaller than the classical probability (horizontal dashed line), but as shown in Fig. 8 for 5.0 kV/cm, for example, the probabilities of finding the carriers in the well region for small energies are on average higher than the classical probability.

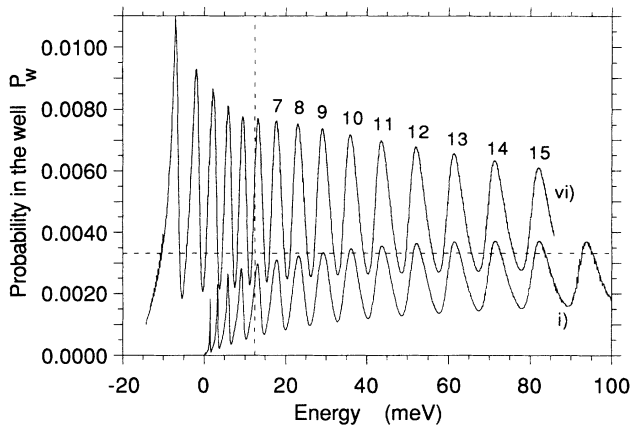

FIG. 8. Comparison between curve i (0 kV/cm) and vi (5.0 kV/cm) of Fig. 7. Curve vi has been shifted in energy to align the peaks which were labeled from 7 to 15. The horizontal dashed line is the classical probability of finding the carrier in the well, and the veritical dashed line indicates the position of the E_0 line for curve vi, as illustrated in 1(b).

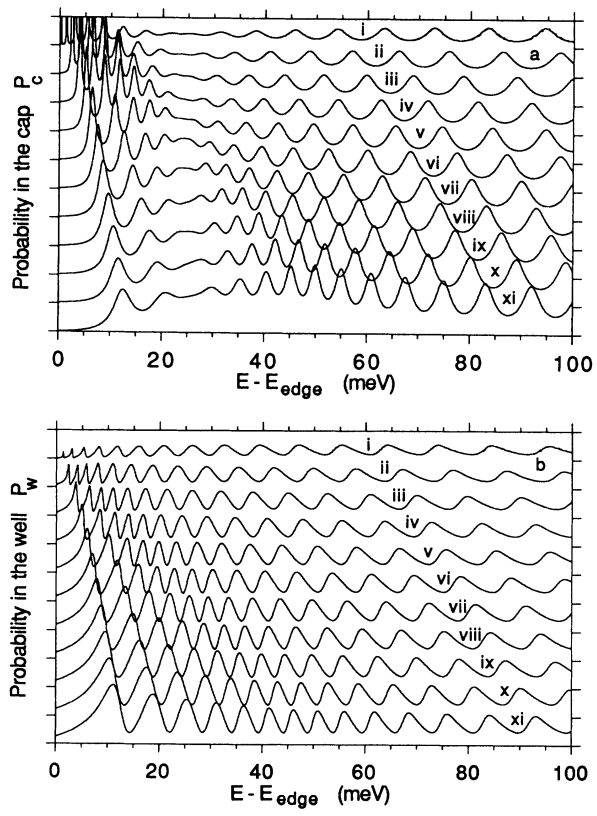

FIG. 7. Normalized probabilities of finding the heavy holes in (a) the cap layer, and (b) in the well for a SQW similar to the one of Fig. 5, for applied electric field from 0 to 10 kV/cm in steps of 1.0 kV/cm corresponding to curves i to xi.

III. DISCUSSION AND CONCLUSION

Moison *et al.*[7] have studied the effect of the cap layer on the bound energy levels in $Ga_xAl_{1-x}As/GaAs$ quantum wells. The blueshift in transitions involving bound states, predicted in Sec. II A for a thin cap layer, was not observed, supposedly because of surface states. The effects of the cap-layer thickness on the continuum states could not be verified since luminescence techniques were used, and luminescence favors the lowest available bound

states. Experiments which are probing preferentially a specific region of the sample (such as modulated reflectance which would be most sensible to the energy variations of the density of carriers in the cap or well layers near the surface) could be more suited to the observation of the carrier segregation among the various regions of the QW structures induced by the finite size of the cap layer. Such experiments could reflect the predicted energy variations of the well occupancy. Oscillatory behavior at above-barrier energies has been observed recently in $GaAs/In_xGa_{1-x}As$ SQW's (Ref. 1) in photoreflectance experiments. These results are in agreement with the theory described in Sec. II B for the continuum states of SQW with the finite cap layer and no applied field. Also, the literature contains examples[8–10] of results which show structures at above-barrier energies in spectra obtained with MQW. If thin cap layers have been used, it is possible that some of these results may incorporate cap-layer effects like the one discussed in Sec. II C for MQW's with a finite cap layer. Experiments have been carried out to verify the effects of an applied electric field on the continuum states of SQW's with thin cap layers. Electroreflectance results[11] at various biases show shifts of the above-barrier peaks with applied field similar to the one predicted in Sec. II D.

In conclusion, the effects on the energy levels of a high potential in the vicinity of a SQW have been studied theoretically. The shifts in energy for the bound states are small for a quantum well at a distance larger than about 10.0 nm (depending on the penetration depth of the wave function) from the high potential. However, the continuum states are strongly affected by such a potential. For the continuum states, oscillations with energy in the probabilities of finding the carriers in the various regions of the device are expected. If there is no applied electric field, the spacing between the extrema of these oscillations is determined mainly by $\sin^2(k_b t)$, where t is the cap-layer thickness; k_b contains m_b^*, the semiconductor effective mass in the cap layer, and E the energy above the barrier. The best contrasts in probabilities are obtained for deep, narrow wells and small effective masses. The contrast in probability is enhanced by the presence of additional wells in the case of MQW's in the same configuration. It was also found that the well(s) nearest to the surface were more energy selective in capturing carriers in the continuum. This may result in different capture efficiencies for the various wells of a MQW structure. If an electric field is applied to the structure, the probability peaks shift linearly in energy with the magnitude of the field when the polarity of the field is such that the potential away from the surface is lowered, and at small energies above the continuum edge, the probability of finding the carriers in the well region increases with the electric field.

ACKNOWLEDGMENTS

I would like to thank the Natural Sciences and Engineering Research Council of Canada for financial support and E. Fortin, G. C. Aers, A. P. Roth, and L. B. Allard for helpful discussions.

[1]S. Fafard, E. Fortin, and A. P. Roth, Phys. Rev. B **45**, 13 769 (1992).

[2]C. Weisbuch, in *Semiconductors and Semimetals,* edited by R. Dingle (Academic, New York, 1987), Vol. 24, Chap. 1.

[3]G. Bastard, *Wave Mechanics Applied to Semiconductor Heterostructures* (Les éditions de Physique, Paris, 1988).

[4]G. Bastard, J. A. Brum, and R. Ferreira, in *Solid State Physics,* edited by H. Ehrenreich and D. Turnbull (Academic, San Diego, 1991), Vol. 44, p. 229ff.

[5]W. Trzeciakowski and M. Gurioli, Phys. Rev. B **44**, 3880 (1991).

[6]*Handbook of Mathematical Functions,* edited by M. Abramowitz and I. A. Stegun (National Bureau of Standards, Washington, D. C., 1964).

[7]J. M. Moison, K. Elcess, F. Houzay, J. Y. Marzin, J. M. Gérald, and M. Bensoussan, Phys. Rev. B **41**, 12 945 (1990).

[8]S. H. Pan *et al.*, Phys. Rev. B **38**, 3375 (1988).

[9]G. Ji, W. Dobbelaere, D. Huang, and H. Morkoç, Phys. Rev. B **39**, 3216 (1989).

[10]R. L. Tober and J. P. Bruno, Proc. SPIE **1286**, 291 (1990).

[11]S. Fafard, E. Fortin, and A. P. Roth (unpublished).